Protection and Control of Modern Power Systems

ORIGINAL RESEARCH Open Access

Communication infrastructure for situational awareness enhancement in WAMS with optimal PMU placement

Bhargav Appasani*, Amitkumar Vidyakant Jha, Sunil Kumar Mishra and Abu Nasar Ghazali

Abstract

Real time monitoring and control of a modern power system has achieved significant development since the incorporation of the phasor measurement unit (PMU). Due to the time-synchronized capabilities, PMU has increased the situational awareness (SA) in a wide area measurement system (WAMS). Operator SA depends on the data pertaining to the real-time health of the grid. This is measured by PMUs and is accessible for data analytics at the data monitoring station referred to as the phasor data concentrator (PDC). Availability of the communication system and communication delay are two of the decisive factors governing the operator SA. This paper presents a pragmatic metric to assess the operator SA and ensure optimal locations for the placement of PMUs, PDC, and the underlying communication infrastructure to increase the efficacy of operator SA. The uses of digital elevation model (DEM) data of the surface topography to determine the optimal locations for the placement of the PMU, and the microwave technology for communicating synchrophasor data is another important contribution carried out in this paper. The practical power grid system of Bihar in India is considered as a case study, and extensive simulation results and analysis are presented for validating the proposed methodology.

Keywords: Situational awareness, Phasor measurement unit, Optimal placement, Microwave communication

1 Introduction

The present day power system is an intricate interconnection of numerous components communicating with each other and has been attributed as the most complex man-made system of the twentieth century [1]. Real-time monitoring and control of these components, distributed over a large topographical sprawl, is a challenging problem for power system engineers. The development of the phasor measurement unit (PMU) can be considered as a breakthrough in this field [2, 3]. Time-synchronized measurement of voltage and current phasors and their subsequent transferal in real time for monitoring and control purposes, are some of the powerful features of the PMU. They empower power system operators with enhanced situational awareness (SA) [4, 5]. Operator SA involves continual monitoring and processing of real-time grid parameters in order to capture the grid dynamics and take necessary control actions, thereby avoiding major power upheavals [6, 7]. SA is largely dependent on the granularity of the sensor measurements, the availability of the communication system, the propagation delay incurred, and the data analytics employed for disturbance detection [8]. Thus, an efficient communication system is an essential requirement in communicating the voluminous real-time data generated at the PMU to the phasor data concentrator (PDC), for enhanced SA [8]. Such a synchrophasor communication system is shown in Fig. 1.

1.1 Contributions

Over the past few decades, many innovative applications and visualization techniques have been developed for enhancing the SA in a wide area measurement system (WAMS) [9–12]. Numerous data mining and data

* Correspondence: appybarkas@gmail.com
School of Electronic Engineering, KIIT University, Bhubaneswar 751024, India

Springer Open

© The Author(s). 2021 **Open Access** This article is licensed under a Creative Commons Attribution 4.0 International License, which permits use, sharing, adaptation, distribution and reproduction in any medium or format, as long as you give appropriate credit to the original author(s) and the source, provide a link to the Creative Commons licence, and indicate if changes were made. The images or other third party material in this article are included in the article's Creative Commons licence, unless indicated otherwise in a credit line to the material. If material is not included in the article's Creative Commons licence and your intended use is not permitted by statutory regulation or exceeds the permitted use, you will need to obtain permission directly from the copyright holder. To view a copy of this licence, visit http://creativecommons.org/licenses/by/4.0/.

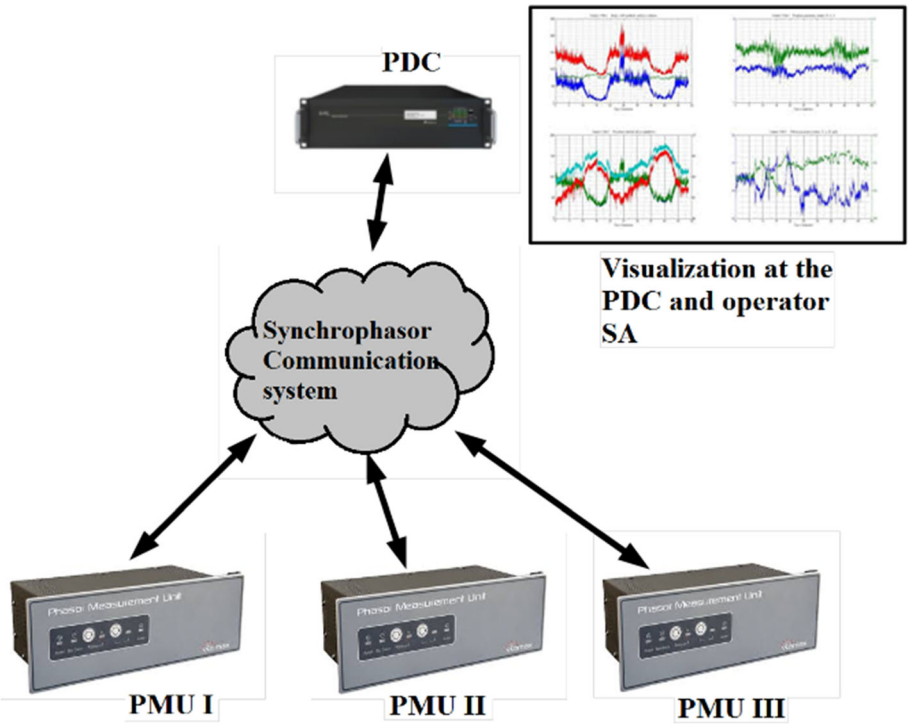

Fig. 1 Synchrophasor communication system and the operator SA

assessment techniques have been developed for improved disturbance detection and the subsequent SA enhancement [13–17]. However, there has been limited study on optimizing the WAMS communication system for SA enhancement. The primary focus of the optimization strategies presented in [18–22] are on improving the availability of a communication system without taking propagation delay into consideration [8]. In this paper, an SA metric in the context of the synchrophasor communication system (SPCS) is presented based on two of the pivotal factors, i.e., propagation delay and communication system availability. Subsequently, the optimal placement of PMUs and communication links is thoroughly investigated for SA enhancement.

Another distinctive feature of this work is the use of a microwave communication system (MCS) to communicate the synchrophasor data between the PMU and the PDC. Over the past few decades, microwave technology has undergone momentous progress in terms of bandwidth and data rates, and has emerged as an alternative to the existing fiber optic technology. Owning to the several advantages of MCS over fiber optic communication, the Power Grid Corporation of India Limited (PGCIL) uses MCS as a substitute for fiber optic communication for communicating synchrophasor data [23]. The most distinct feature of this technology is that the data can be communicated 40% faster than the existing fiber optic communication, and hence it can enhance operator SA [24].

Microwave technology needs a clear line of sight (LoS) between the transmitting and receiving antennas. The existence of LoS between the communicating devices that are topographically separated by large distances is not always feasible. To overcome this problem, microwave repeaters are used at regular intervals. The deployment of intermediate repeaters also improves the link availability and the quality of the received signal. Hence, proper placement of the intermediate repeaters is a requirement for reliable synchrophasor data communication. This requires knowledge of the Earth's topography, which is available in the form of Digital elevation model (DEM) data. In [25], an automatic repeater placement algorithm based on global 30 arc-second elevation (GTOPO30) DEM data is proposed for minimizing risk. This determines the geographical locations and tower heights for the intermediate repeaters provided that the information about the PMU and the PDC is known. The main contributions of this work lie in the use of this repeater placement algorithm and the multi-objective Genetic Algorithm (GA) to determine the optimum locations for the PMUs and PDC for operator SA enhancement, while ensuring the system's full observability with the minimum possible number of PMUs. It also uses a bio-geography based optimization (BBO) algorithm for optimizing the tower heights [26], while

the effect of zero injection measurements on the network SA is also analyzed.

1.2 Organization of the paper

The rest of the paper is organized as follows. Section 2 discusses a brief overview of the microwave communication system to facilitate PMU data transfer. The various components of the system essential to evaluate availability are also described. An SA assessment metric in the context of the synchrophasor communication system is presented in Section 3. The automatic repeater placement algorithm aided by multi-objective GA for the optimal placement of both PMUs and PDC is presented in Section 4. Using the GTOPO30 DEM data, the location of the repeaters, the propagation delay, the system availability, and the ensuing SA for the optimum configuration are also evaluated in Section 4. The simulation results for the case study are discussed and analyzed in Section 5 and the conclusion of the work is drawn in Section 6.

2 Microwave communication system for PMU data transfer

Microwave-based communication is based on signals having frequencies of the order of 3 GHz to 300 GHz. Recently, the bloom of microwave technology transformed it into a potent synchrophasor communication technology, which is now being referred to as a microwave synchrophasor communication system (MSCS). The chief components of an MSCS [25, 27] are the PMU and PDC radios, the connecting cables, microwave repeaters, and antennas, as illustrated in Fig. 2.

The PMU generates time-synchronized data for voltage and current phasors that are modulated by the PMU radio terminal. These are fed to a microwave antenna for transmission. At the PDC, the microwave antenna receives the electromagnetic signals and converts them back into electrical signals. The demodulation at the PDC is carried out by the PDC radio terminal while the demodulated data is used for the ensuing data analytics. Similarly, the command signals sent by the PDC are received by the PMU radio terminal and are demodulated for executing the control actions. In a typical WAMS, the PMU and PDC are geographically separated by hundreds of kilometers and hence intermediate microwave repeaters are used to accomplish data transferal [28].

In this paper, we assume that the synchrophasor communication takes place in the *L6* band that occupies the frequency spectrum in the range of 5.925–6.425 GHz. The maximum distance between the adjacent microwave towers is considered to be 25 Km. This gives a link availability of 0.999999 for communication in the *L6* band [29]. By employing frequency diversity schemes, the availability can be further enhanced and the communication link can be considered to be available throughout the machine operation time [30]. Coaxial connectors are passive components having a low rate of failure, and thus can be omitted from the reliability analysis. The mean time to failure (MTTF) for some of the key components and their mean time to repair (MTTR) are summarized in Table 1 [25].

In the frequency diversity scheme, two radios operating at separate frequencies 'f_1' and 'f_2' are used. This also gives a redundant PMU and PDC radio terminal. Similarly, a (1 + 1) redundant configuration is employed for the microwave repeater, while all the MCSs used in this work have a similar component redundancy as illustrated in Fig. 3.

2.1 Availability analysis

An important process in the design of an engineering system is its availability analysis. In this subsection the basics of availability analysis are presented, as they are important for assessment of operator SA. For a repairable system, the availability can be calculated using (1) [31]. The block diagram of an '*r*' components series system is shown in Fig. 4a and that of an '*r*' component

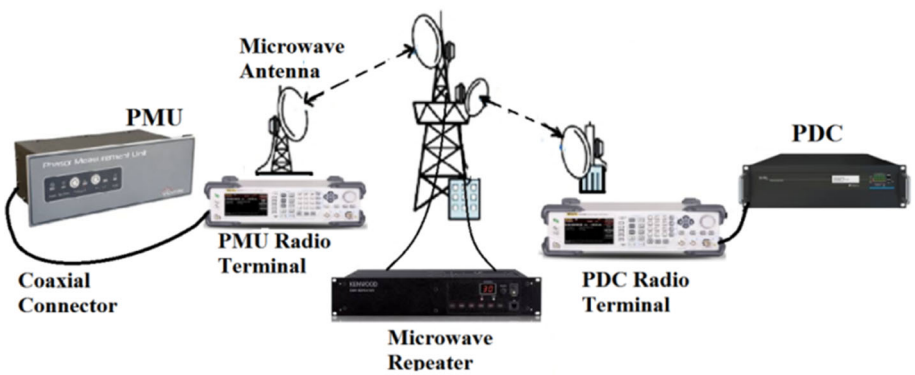

Fig. 2 Basic components of a MSCS

Table 1 The MTTF and MTTR of the constituent components

Components	MTTF (hours)	MTTR (hours)
PMU Radio	175,200	4.5
Microwave Repeater	85,000	4.5
PDC Radio	175,200	4.5
Antenna	2,881,844.34	24

parallel system is depicted in Fig. 4b. Their availabilities can be calculated using Eqs. (2) and (3) respectively.

$$A = \frac{MTTF}{MTTF + MTTR} \tag{1}$$

$$A_{series} = 1 - \sum_{i=1}^{r}\left(\frac{MTTR_i}{MTTR_i + MTTF_i}\right) \tag{2}$$

$$A_{parallel} = 1 - \prod_{i=1}^{r}\left(\frac{MTTR_i}{MTTR_i + MTTF_i}\right) \tag{3}$$

where '$MTTF_i$' and '$MTTR_i$' represent the mean time to failure of the i^{th} component of the system and its corresponding mean time to repair respectively.

From Fig. 3, it can be inferred that an 'N' repeater PMU MCS consists of a single PMU radio terminal subsystem consisting of two radio terminals operating in parallel. Similarly, it also has a single PDC radio terminal subsystem consisting of two radio terminals operating in parallel, '$2N + 2$' antennas and 'N' repeaters operating in series with the radio terminal subsystems and 'N' repeater subsystems each consisting of two repeaters operating in parallel. The series parallel block diagram for an MSCS with single repeater is depicted in Fig. 5 to illustrate the concept. Further, this will also aid in elucidating the general expression indicating the availability of an 'N' repeater MSCS which is given by Eq. (4).

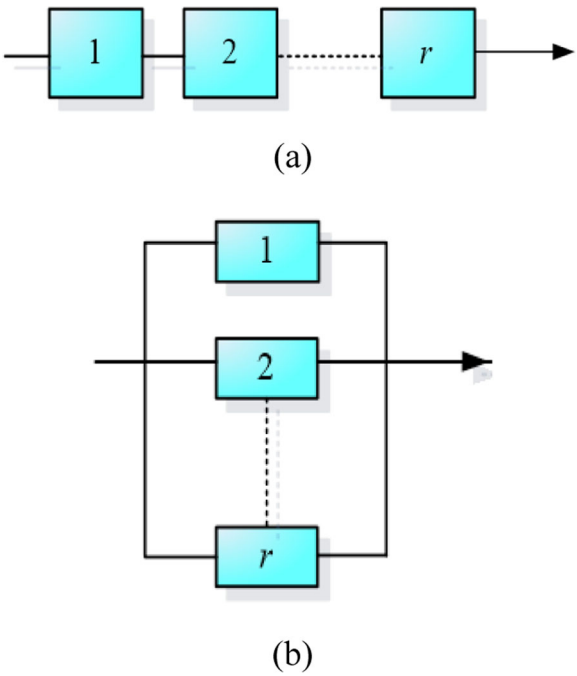

Fig. 4 Block diagram of **a** Series system **b** Parallel system

$$A(N) = 1 - \{U_{PMU\ -\ radio} + N\,U_{repeater} + U_{PDC\ -\ radio} + (2 \times N + 2)U_{antenna}\} \tag{4}$$

where,

$U_{PMU\ -\ radio} = \left(\frac{MTTR_{PMU\ -\ radio}}{MTTF_{PMU\ -\ radio} + MTTR_{PMU\ -\ radio}}\right)^2$ represents the unavailability for both PMU radio terminals.

$U_{repeater} = \left(\frac{MTTR_{repeater}}{MTTF_{repeater} + MTTR_{repeater}}\right)^2$ represents the unavailability of both repeaters.

$U_{PDC\ -\ radio} = \left(\frac{MTTR_{PDC\ -\ radio}}{MTTF_{PDC\ -\ radio} + MTTR_{PDC\ -\ radio}}\right)^2$ represents the unavailability of both PDC radio terminals.

$U_{antenna} = \left(\frac{MTTR_{antenna}}{MTTF_{antenna} + MTTR_{antenna}}\right)$ represents the unavailability of both antennas.

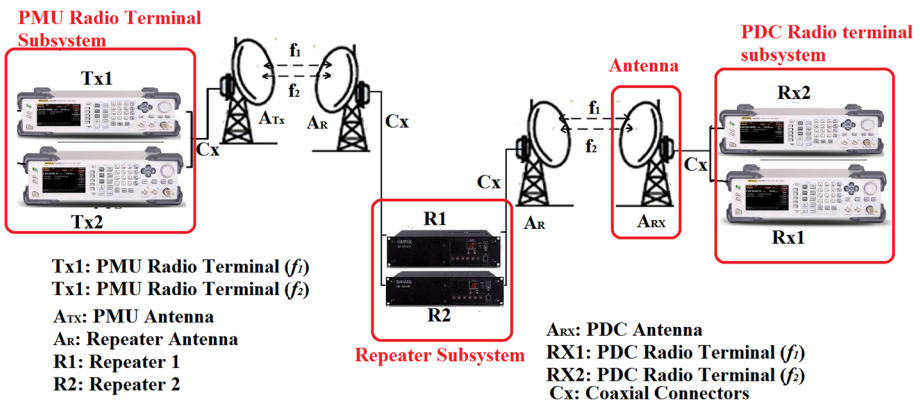

Fig. 3 A single repeater PMU MCS

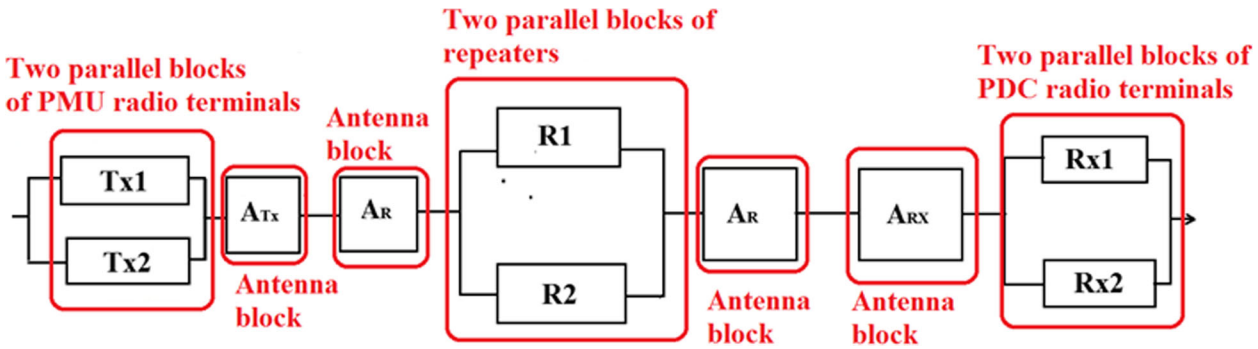

Fig. 5 Series-parallel block diagram

3 SA assessment metric

For a synchrophasor communication system, propagation delay and network availability play pivotal roles in determining the operator SA. These should be taken account of in the assessment metric. A pragmatic expression for the operator SA can be represented as:

$$SA = \frac{1}{1 + (T_p/T_s)} A \tag{5}$$

where T_p is the propagation delay, and A represents the availability of the MSCS for the PMU and PDC link. This is evaluated using (4). T_s represents the processing delay due to the time required by the PMU and PDC to process the data. The standard value of processing delay is considered to be 75 ms [32].

The normalized factor (T_p/ T_s) ensures that the SA is a unit-less quantity and the summation in the denominator retains the SA within the range of 0 to 1. When the propagation delay is zero the operator SA is determined by the availability of the communication system, and when the delay is infinity SA becomes zero. Thus the expression can be considered as a good estimate of the operator SA. Based on the metric given in (5) and from the permissible delays for the various synchrophasor applications, the SA metric for various PMU applications is reported in Table 2 [33].

For a power system consisting of 'NPMU' PMUs, the operator SA for the overall system can be obtained as:

$$SA_{system}^{mean} = \frac{1}{N_{PMU}} \sum_{t=1}^{N_{PMU}} SA_t \tag{6}$$

where SA_t is the SA evaluated for the t^{th} PMU-PDC pair MSCS. If the PMU and PDC are co-located on the same electrical bus, the operator SA for that PMU-PDC pair is taken as unity.

Another pragmatic expression, which can be used as a measure for evaluating the system operator SA, is given by:

$$SA_{system}^{\min} = \min(SA_t) \forall t = 1, 2, ..., N_{PMU} \tag{7}$$

The theoretical aspects of availability evaluation and SA assessment have been described, as in (5)–(7). These equations show that the availability evaluation and SA assessment depends on the number of repeaters deployed between the PMU and PDC to establish a reliable communication system. In the next section, the automatic repeater placement algorithm is presented to aid the construction and evaluation of the system SA.

4 Optimal placement of PMUs for SA enhancement

The PMU and its MCS are the expensive units, and so this necessitates judicial use of these devices. To obtain the time-synchronized data of voltage and current phasors, it is not necessary to place PMUs on every electrical bus in the network. A PMU placed on a particular bus measures its voltage phasors and simultaneously the current phasors of all the incident lines [34]. Therefore, using the network equations, one can obtain the voltage phasors of all the buses connected to the PMU equipped bus. Hence, by placing PMUs at optimal locations in the

Table 2 Communication delays for various PMU applications

PMU Application	Communication Delay (*msec*)	SA
State Estimation	100	0.75
Oscillation control	200	0.375
Damping control	200	0.375
Voltage angle control	100	0.75
Frequency deviation control	100	0.75

network it is possible to observe the entire network. The problem of optimal placement of PMUs has received considerable attention and a plethora of literature is available on this topic. An excellent review of these techniques is given in [35]. In the present work, a binary linear programming-aided [36, 37] multi-objective GA [38] is used to find the optimal coordinates to locate both PMUs and PDC. This algorithm ensures that the entire power system is observable with maximum system SA using the least number of PMUs.

Consider a power grid system consisting of '*b*' buses and '*l*' branches. The connectivity matrix '**P**', which is a square matrix of order *b*, is used to expresses their connectivity. The elements of this connectivity matrix 'P' can be determined using Eq. (8).

$$p_{uv} = \left\{ \begin{array}{l} 1 \text{ if } \exists \text{a connection between u}^{th} \text{ bus and v}^{th} \text{ bus; or if u} = \text{v} \\ 0 \text{ otherwise} \end{array} \right\} \tag{8}$$

Likewise, the location of the PMUs for the considered system can be determined by a column matrix '**Q**', having *b* rows. The elements of the matrix '**Q**' are represented as:

$$q_u = \left\{ \begin{array}{l} 1 \text{ if } \exists a \text{ PMU on the u}^{th} \text{ bus} \\ 0 \text{ otherwise} \end{array} \right\} \tag{9}$$

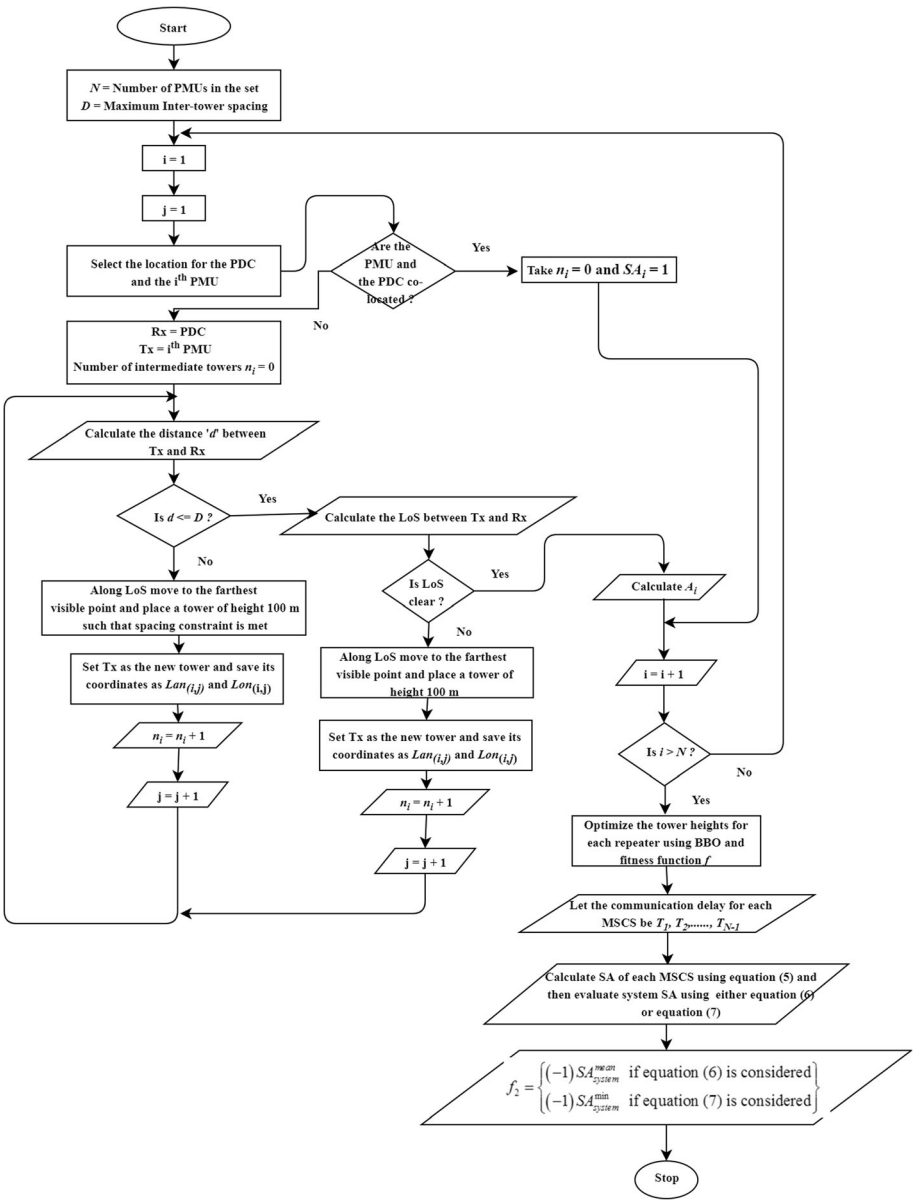

Fig. 6 Flow chart for SA evaluation

When a bus is neither connected to a load nor to a generator, the sum of all currents associated with the branches connected to the bus is zero, and thus such a bus is called a zero injection bus (ZIB). Including the ZIBs reduces the number of PMUs required to achieve system observability. This is the first parameter to be optimized as given by [37]:

$$F_1 = \sum_{u=1}^{b} q_u \tag{10}$$

$$\text{S.T.} \left\{ \begin{array}{ll} \mathbf{PQ} \geq \mathbf{b_1} & \text{if ZIBs are considered} \\ \mathbf{T_{con} P_1 PQ} \geq \mathbf{b_2} & \text{if ZIBs are not considered} \end{array} \right\}$$

where, $\mathbf{b_1} = [1\ 1 \ldots\ldots 1]^T_{(b\times 1)}$, $\mathbf{T_{con}} = \begin{bmatrix} I_{B\times B} & 0 \\ 0 & \mathbf{T_{mes}} \end{bmatrix}$, $\mathbf{P_1}$ is the permutation matrix and '*B*' is the number of buses not associated with ZIBs. The details regarding the construction of these matrices will be explained with the help of the case study in the next section.

The measure of the system SA is the second function to be optimized. For optimization, the multi-objective GA algorithm is used. It is given by Eq. (11).

$$F_2 = \left\{ \begin{array}{ll} (-1) SA_{system}^{mean} & \text{if equation (6) is considered as SA metric} \\ (-1) SA_{system}^{\min} & \text{if equation (7) is considered as SA metric} \end{array} \right\} \tag{11}$$

In order to calculate the system SA, we first need to determine the PDC location and then find out the required number of repeaters to achieve the communication feasibility for every PMU and the PDC. Thus, the system SA is affected by the location of the PMUs and PDC. The multi-objective GA places the PMUs and PDC such that the system SA is also maximized. For determining the number of repeaters required to establish the MSCS for each PMU and PDC, an automatic repeater placement algorithm is used. This is based on GTOPO30 DEM data [25]. The DEM data gives the information of the Earth's topography and aids in the repeater placement for establishing an efficient MCS infrastructure. The placement of the repeaters is on the basis of existence of LoS and on the inter-tower distances. Further, the BBO algorithm is used to optimize the heights of the towers, such that the propagation delay is minimized. The system SA is then evaluated and finally, the optimum configuration is determined. The automatic repeater placement algorithm to calculate the system SA is illustrated using a flow chart depicted in Fig. 6.

It is worth mentioning that the propagation delay in MSCS is dependent on the heights of the towers and the corresponding locations of the repeaters. To minimize the propagation delay, it is pertinent to optimize the heights of the microwave towers. Thus, prior to evaluating the SA, the BBO algorithm is used to optimize these heights. The objective function considered for optimizing is represented by Eq. (12).

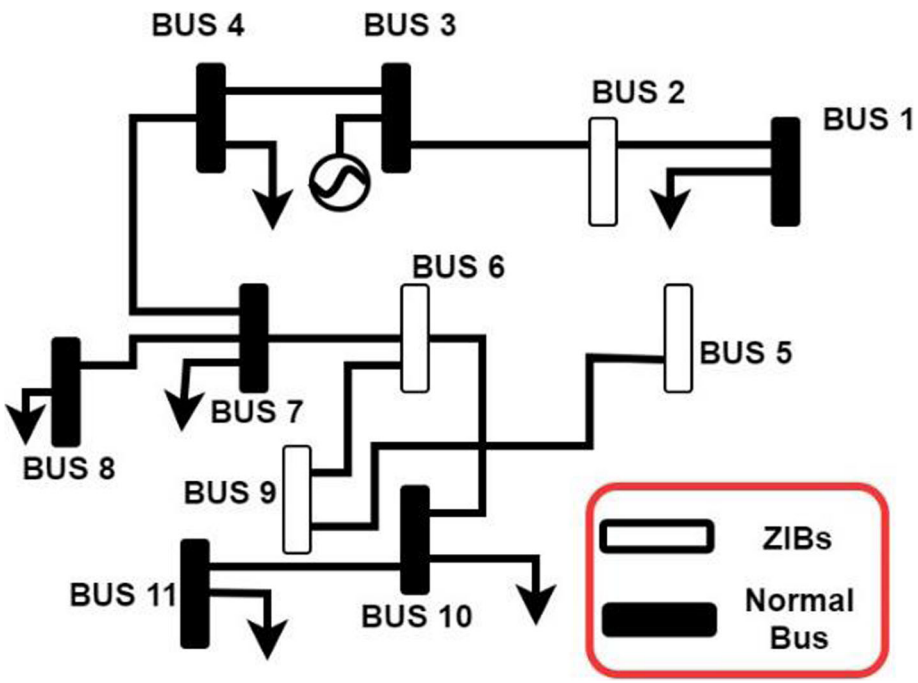

Fig. 7 Single Line Diagram of the Bihar Power Grid (including all buses), India [25]

Table 3 Locations of different buses for the Bihar power grid

Bus Number	Bus Location (City)	Latitude (°N)	Longitude (°E)
2	Begusarai	25.2446	86.0734
6	Biharshariff-I	25.2709	85.3206
9	Biharshariff-II	25.2218	85.3138
11	Dehri	24.5300	84.1309
7	Fatuah	25.3105	85.1911
10	Gaya	24.4758	85.0055
4	Hazipur	25.4900	85.2327
5	Kahalgaon	24.5129	87.3637
3	Muzaffarpur	26.0849	85.2134
8	Patna	25.3649	85.0751
1	Purnea	25.4647	87.2822

$$f = LoS = \sum_{m=1}^{G-1}\left(\sqrt{d_m^2 + ((ml_{m+1} + H_{m+1}) - (ml_m + H_m))^2}\right) \quad (12)$$

where G is the number of towers, d_m is the distance between the m^{th} and its next i.e., $(m+1)^{th}$ tower (in meters), ml_m and H_m are the mean sea level height and the height of the m^{th} tower (in meters), respectively.

According to [32], an excess delay considered for each repeater is equal to approximately 150 ns. Therefore, Eq. (13) can be used to describe the propagation delay incurred for the synchrophasor communication between the k^{th} PMU and the PDC.

$$T_k = \frac{LoS_k}{3 \times 10^5} + 0.15a_k \text{ (ms)} \quad (13)$$

where LoS_k is the Line of Sight distance for the k^{th} PMU and PDC determined from (12), and a_k is the number of repeaters required for a MCS link connecting the k^{th} PMU and PDC. This number is obtained using the DEM data.

5 Case studies

As a case study, the practical power grid system of Bihar, India is considered for validating the proposed methodology [28]. The one-line diagram of the considered power grid system is as depicted in Fig. 7. The DEM-based automatic repeater placement algorithm is implemented using MATLAB and the simulations for the system under consideration are performed. For the electrical buses considered in this system, their corresponding geographical locations (coordinates) are given in Table 3. This practical power grid consisting of 11 buses was chosen as it is feasible to elucidate the details involved in the proposed methodology.

5.1 Without ZIB measurements

First we consider when the ZIBs are not included in the optimization process and the Eq. (6) is considered as the SA metric for evaluating the second objective function 'F_2'. The parameters of the multi-objective GA for the optimization are as follows: mutation rate = 0.01, number of generations = 100, and elite count = 2.

Table 4 Case study results without ZIB measurements

	For PMU located on Bus 2 and PDC located on Bus 9, estimation of MSCS			For PMU located on Bus 7 and PDC located on Bus 9, estimation of MSCS			For PMU located on Bus 10 and PDC located on Bus 9, estimation of MSCS		
	Latitude(°N)	Longitude (°E)	Tower heights (m)	Latitude (°N)	Longitude (°E)	Tower heights (m)	Latitude (°N)	Longitude (°E)	Tower heights (m)
PMU Radio Terminal	25.2446	86.0734	100	25.3105	85.1911	97.06	24.4758	85.0055	50.51
Repeater 1	25.2376	85.8276	98.95	–	–	–	24.6847	85.0915	99.87
Repeater 2	25.2303	85.5819	100	–	–	–	24.8936	85.1777	89.91
Repeater 3	25.2225	85.3361	99.5	–	–	–	25.1025	85.2642	96.18
PDC Radio	25.2218	85.3138	97.88	25.2218	85.3138	95.12	25.2218	85.3138	100
Number of Repeaters required	3			0			3		
Prop. Delay (*ms*)	0.2548			0.0527			0.2953		
Availability	0.999933372157467			0.999983344151698			0.999933372157467		
SA	0.996547497605291			0.999281802527150			0.996011636292648		
System SA Metric: SA_{system}^{mean}	**(0.996547497605291 + 0.999281802527150 + 0.996011636292648 + 1)/4 = 0.997960234106272**								
System SA Metric: SA_{system}^{min}	**Min(0.996547497605291, 0.999281802527150, 0.996011636292648, 1) = 0.996011636292648**								

The optimal locations for the placement of different PMUs are obtained as follows: bus 2 (*Begusarai*), bus 9 (*Biharshariff*-II), bus 7 (*Fatuah*), and bus 10 (*Gaya*). Moreover, the bus 9 (*Biharshariff*-II) is found to be the optimum location of the PDC. This system has resulted in the maximum system SA metric, SA_{system}^{mean} of 0.997280312141696. When the second SA metric is chosen for evaluating the second objective function 'F_2', the optimum locations for the PMU and PDC placement are again found to be the same with the maximized system SA metric, $SA_{system}^{\min}$ of 0.996011636292648. The results of this case study without including ZIB measurements are shown in Table 4.

It can be further observed from the results reported in Table 4 that if the number of intermediate repeaters are reduced, the availability of the communication system increases and propagation delay reduces, thereby increasing the operator SA. In some cases, because of the geographical profile, additional repeaters may be needed to maintain LoS. This reduces the communication system availability but does not affect the propagation delay.

5.2 With ZIB measurements

Buses 2, 5, 6 and 9 do not have any generator or load and hence can be considered as ZIBs. First we construct the matrices $\mathbf{T_{con}}$, $\mathbf{T_{mes}}$, $\mathbf{P_1}$ and $\mathbf{b_2}$ for the presented case study and incorporate them for evaluating the objective function 'F_1'.

We can see that buses 4, 8 and 11 are not associated with any ZIBs, and therefore $B = 3$. There are injection measurements at buses 2, 5, 6 and 9. Therefore, we have:

$$\mathbf{T_{mes}} = \begin{bmatrix} 1 & 0 & 1 & 0 & 0 & 0 & 0 & 0 \\ 0 & 0 & 0 & 0 & 0 & 0 & 0 & 1 \\ 0 & 0 & 0 & 0 & 0 & 1 & 1 & 1 \\ 0 & 0 & 0 & 1 & 1 & 0 & 0 & 0 \end{bmatrix} \begin{matrix} \text{injection measurement at 2} \\ \text{injection measurement at 5} \\ \text{injection measurement at 6} \\ \text{injection measurement at 9} \end{matrix}$$

$$Bus\#\ 1\ 2\ 3\ 5\ 6\ 7\ 9\ 10$$

The permutation matrix and matrix b_2 can be written [39] as:

$$\mathbf{P_1} = \begin{bmatrix} 0 & 0 & 0 & 1 & 0 & 0 & 0 & 0 & 0 & 0 & 0 \\ 0 & 0 & 0 & 0 & 0 & 0 & 0 & 1 & 0 & 0 & 0 \\ 0 & 0 & 0 & 0 & 0 & 0 & 0 & 0 & 0 & 0 & 1 \\ 1 & 0 & 0 & 0 & 0 & 0 & 0 & 0 & 0 & 0 & 0 \\ 0 & 1 & 0 & 0 & 0 & 0 & 0 & 0 & 0 & 0 & 0 \\ 0 & 0 & 1 & 0 & 0 & 0 & 0 & 0 & 0 & 0 & 0 \\ 0 & 0 & 0 & 0 & 1 & 0 & 0 & 0 & 0 & 0 & 0 \\ 0 & 0 & 0 & 0 & 0 & 1 & 0 & 0 & 0 & 0 & 0 \\ 0 & 0 & 0 & 0 & 0 & 0 & 1 & 0 & 0 & 0 & 0 \\ 0 & 0 & 0 & 0 & 0 & 0 & 0 & 0 & 1 & 0 & 0 \\ 0 & 0 & 0 & 0 & 0 & 0 & 0 & 0 & 0 & 1 & 0 \end{bmatrix} \begin{matrix} Bus\ 4 \\ Bus\ 8 \\ Bus\ 11 \\ Bus\ 1 \\ Bus\ 2 \\ Bus\ 3 \\ Bus\ 5 \\ Bus\ 6 \\ Bus\ 7 \\ Bus\ 9 \\ Bus\ 10 \end{matrix} \quad \mathbf{b_2} = [1\ \ 1\ \ 1\ \ 1\ \ 0\ \ 2\ \ 1]^T$$

Now, the T_{con} can be written as:

$$\mathbf{T_{con}} = \begin{bmatrix} I_{B\times B} & 0 \\ 0 & \mathbf{T_{mes}} \end{bmatrix} = \left[\begin{array}{ccc|ccccccccc} 1 & 0 & 0 & 0 & 0 & 0 & 0 & 0 & 0 & 0 & 0 \\ 0 & 1 & 0 & 0 & 0 & 0 & 0 & 0 & 0 & 0 & 0 \\ 0 & 0 & 1 & 0 & 0 & 0 & 0 & 0 & 0 & 0 & 0 \\ \hline 0 & 0 & 0 & 1 & 0 & 1 & 0 & 0 & 0 & 0 & 0 \\ 0 & 0 & 0 & 0 & 0 & 0 & 0 & 0 & 0 & 1 & 0 \\ 0 & 0 & 0 & 0 & 0 & 0 & 0 & 0 & 1 & 1 & 1 \\ 0 & 0 & 0 & 0 & 0 & 0 & 1 & 1 & 0 & 0 & 0 \end{array}\right]$$

The results of the case study with the ZIB measurements included are shown in Table 5 and the summary of the results with and without the inclusion of ZIB measurements are compared in Table 6.

The optimum location of the PMUs with ZIBs included and with the objective function 'F_2' evaluated using (6) are buses 2 (*Begusarai*), bus 10 (*Gaya*), and bus 7 (*Fatuah*). The optimal location for placement of

Table 5 Case study results with ZIB measurements

	For PMU located on Bus 2 and PDC located on Bus 9, estimation of MSCS			For PMU located on Bus 7 and PDC located on Bus 9, estimation of MSCS			For PMU located on Bus 10 and PDC located on Bus 9, estimation of MSCS		
	Latitude (°N)	Longitude (°E)	Tower heights (m)	Latitude (°N)	Longitude (°E)	Tower heights (m)	Latitude (°N)	Longitude (°E)	Tower heights (m)
PMU Radio Terminal	25.2446	86.0734	100	25.3105	85.1911	97.06	24.4758	85.0055	50.51
Repeater 1	25.2376	85.8276	98.95	–	–	–	24.6847	85.0915	99.87
Repeater 2	25.2303	85.5819	100	–	–	–	24.8936	85.1777	89.91
Repeater 3	25.2225	85.3361	99.5	–	–	–	25.1025	85.2642	96.18
PDC Radio	25.2218	85.3138	97.88	25.2218	85.3138	95.12	25.2218	85.3138	100
No. of Repeaters required	3			0			3		
Propagation delay measured in *ms*	0.2548			0.0527			0.2953		
Availability	0.999933372157467			0.999983344151698			0.999933372157467		
SA	0.996547497605291			0.999281802527150			0.996011636292648		
System SA Metric: SA_{system}^{mean}	**(0.996547497605291 + 0.999281802527150 + 0.996011636292648)/3 = 0.997280312141696**								
System SA Metric: $SA_{system}^{\min}$	**Min(0.996547497605291, 0.999281802527150, 0.996011636292648) = 0.996011636292648**								

Table 6 A summary of the case studies

Case study	ZIB measurements included? (yes/no)	System SA metric considered	Optimum locations of PMUs (Bus Nos)	Optimum location of PDC (Bus No)	System SA
I	No	SA_{system}^{mean}	2, 7, 9, 10	9	0.997960234106272
II	No	SA_{system}^{min}	2, 7, 9, 10	9	0.996011636292648
III	Yes	SA_{system}^{mean}	2, 7, 10	9	0.997280312141696
IV	Yes	SA_{system}^{min}	2, 7, 10	9	0.996011636292648

the PDC is bus 9 (*Biharshariff*-II) with the maximized system SA metric SA_{system}^{mean} of 0.997280312141696. When the objective function 'F_2' is evaluated using (7), the optimal locations of the PMUs and PDC remain the same while the obtained maximized SA_{system}^{min} is 0.996011636292648.

It can be noted that inclusion of the ZIB measurements minimizes the number of PMUs needed for observing the system and at the same time it has not greatly affected the operator SA. Reducing the number of PMUs reduces the overall cost of the monitoring system so inclusion of ZIB measurements is desirable. Furthermore, from the SA calculated in Table 2, it can be observed that the achieved SA using the proposed method is satisfactory for most of the PMU applications.

5.3 Validation of results

In order to validate these results for LoS and link availability, each of the microwave links between the PMU and corresponding PDC is simulated using Atoll, which is a wireless link planning software. For the PMU located at bus 2 (*Begusarai*) and the PDC located at bus 9 (*Biharshariff*-II), microwave P2P links along with the intermediate repeaters in Atoll are shown in Fig. 8.

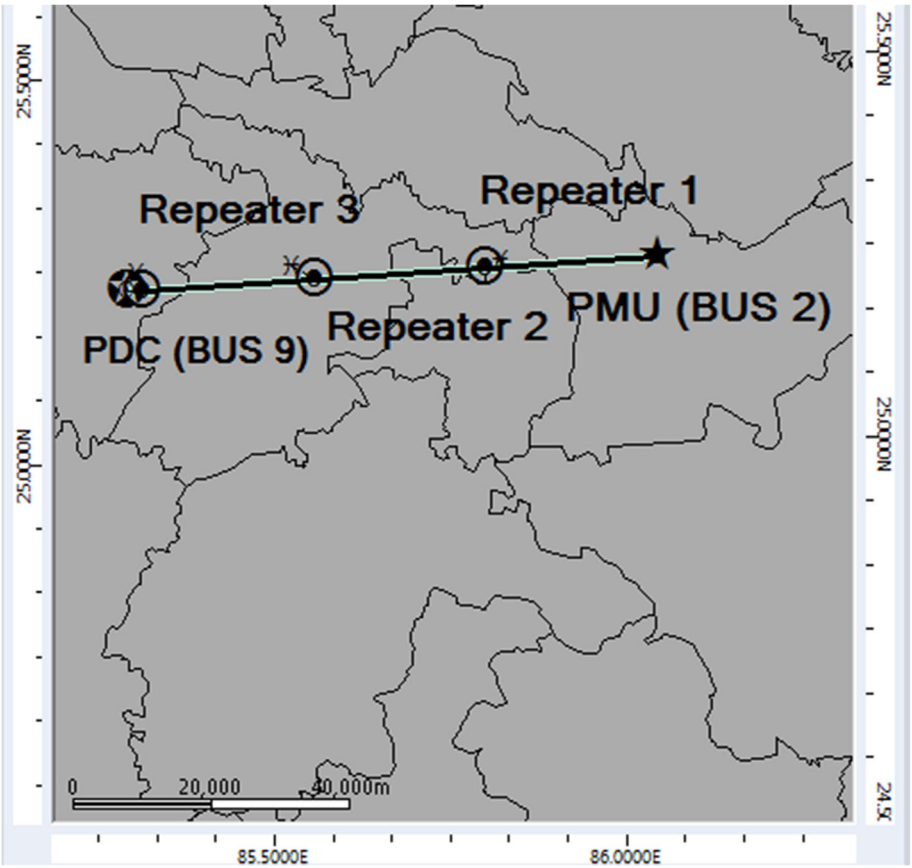

Fig. 8 The MSCS for the PMU located on bus 2 and the PDC located on bus 9 for the case study

6 Conclusion

SA enhancement has been a challenge to power system engineers. A pragmatic expression for evaluating the SA in the framework of the synchrophasor communication system would be of great aid in the design of an optimal situational awareness system. Operator SA can be augmented using optimal placement of the PMUs with respect to the PDC. Two metrics for evaluating the SA have been presented along with the optimal placement of the PMUs, the PDC and corresponding microwave synchrophasor communication system for one of the practical power grid systems of India to substantiate the proposed methodology. The authors would like to include economic considerations into the analysis in their future work.

Abbreviations

BBO: Bio-geography based optimization; DEM: Digital elevation model; GA: Genetic algorithm; LoS: Line of sight; MCS: Microwave communication system; MTTF: Mean time to failure; MTTR: Mean time to repair; MSCS: Microwave synchrophasor communication system; PDC: Phasor data concentrator; PGCIL: Power Grid Corporation of India Limited; PMU: Phasor measurement unit; SA: Situational awareness; SPCS: Synchrophasor communication system; WAMS: Wide area measurement system; ZIB: Zero injection bus

Acknowledgments

Not Applicable.

Authors' contributions

Bhargav Appasani: Simulation Work. Amitkumar Vidyakant Jha: Writing and Organizing. Sunil Kumar Mishra: Figures and literature review. Abu Nasar Ghazali: Main idea and co-ordinating others. The author(s) read and approved the final manuscript.

Funding

Not Applicable.

Availability of data and materials

All the relevant data has been provided in the main manuscript.

Declarations

Competing interests

The authors do not have any competing interests.

Received: 3 January 2020 Accepted: 22 February 2021
Published online: 23 March 2021

References

1. Bobba, R. B., et al. (2012). Enhancing grid measurements. *IEEE Power Energy Magazine*, *10*(1), 67–73.
2. Phadke, A. G., & Thorp, J. S. (2008). Phasor measurement units and phasor data concentrators. In *Synchronized phasor measurements and its applications*, (pp. 93–105). New York, Chap.5: Springer.
3. Ree, J. D. L., et al. (2010). Synchronized phasor measurement applications in power system. *IEEE Transactions on Smart Grid*, *1*(1), 20–27.
4. Gopakumar, P., Reddy, M. J. B., & Mohanta, D. K. (2015). Fault detection and lo-calization methodology for self-healing in smart power grids incorporating phasor measurement units. *Electric Power Components and Systems*, *43*(6), 695–710.
5. Gopakumar, P., Reddy, M. J. B., & Mohanta, D. K. (2015). A novel topological genetic algorithm-based phasor measurement unit placement and scheduling methodology for enhanced state estimation. *Electric Power Components and Systems*, *43*(16), 1843–1858.
6. Panteli, M., & Kirschen, D. (2015). Situation awareness in power systems: Theory, challenges and applications. *Electric Power Systems Research*, *122*, 140–151.
7. Panteli, M., et al. (2013). Assessing the impact of insufficient situation awareness on power system operation. *IEEE Transactions on Power Systems*, *28*(3), 2967–2977.
8. Brahma, S., Kavasseri, R., et al. (2017). Real-time identification of dynamic events in power systems using PMU data, and potential applications—Models, promises, and challenges. *IEEE Transactions on Power Delivery*, *32*(1), 294–301.
9. Zhang, G., Sun, K., et al. (2011). *Application of synchrophasor measurements for improving operator situational awareness*, (pp. 1–8). San Diego: IEEE Power and Energy Society General Meeting.
10. Zhang, G., Beard, L., et al. (2009). WAVA- PMU and near real-time event replay using synchrophasor measurements. In *NASPI meeting at Chattanooga*.
11. Parashar, M., & Mo, J. (2009). Real time dynamics monitoring system (RTDMS): Phasor applications for the control room. In *42nd Hawaii international conference on system sciences*.
12. Zhang, G., Lee, S., et al. (2010). *Wide area power system visualization using real-time synchrophasor measurements*. Minneapolis: PES General Meeting.
13. Rafferty, M., et al. (2017). Real-time multiple event detection and classification using moving window PCA. *IEEE Transactions on Smart Grid*, *7*(5), 2537–2548.
14. Liu, X., Laverty, D. M., et al. (2015). Principal component analysis of wide-area phasor measurements for islanding detection—A geometric view. *IEEE Transactions on Power Delivery*, *30*(2), 976–985.
15. Jiang, H., Dai, X., et al. (2016). Spatial-temporal synchrophasor data characterization and analytics in smart grid fault detection, identification, and impact causal analysis. *IEEE Transactions on Smart Grid*, *7*(5), 2525–2536.
16. Wang, B., Fang, B., et al. (2016). Power system transient stability assessment based on big data and the core vector machine. *IEEE Transactions on Smart Grid*, *7*(5), 2561–2570.
17. Hu, J., & Vasilakos, A. V. (2016). Energy big data analytics and security: Challenges and opportunities. *IEEE Transactions on Smart Grid*, *7*(5), 2423–2436.
18. Huang, J., Wu, N. E., & Ruschmann, M. C. (2014). Data-availability-constrained placement of PMUs and communication links in a power system. *IEEE Systems Journal*, *8*(2), 483–492.
19. Wang, Y., Wang, C., et al. (2014). Reliability-based incremental PMU placement. *IEEE Transactions on Power Systems*, *29*(6), 2744–2752.
20. Haghighatdar, F. F., Hooshmand, R. A., & Khodabakhshian, A. (2014). Simultaneous optimal design of measurement and communication infrastructures in hierarchical structured WAMS. *IEEE Transactions on Smart Grid*, *5*(1), 312–319.
21. Shahraeini, M., Ghazizadeh, M. S., & Javidi, M. H. (2012). Co-optimal placement of measurement devices and their related communication infrastructure in wide area measurement systems. *IEEE Transactions on Smart Grid*, *3*(2), 684–691.
22. Yu, W., Luo, J., Xue, Y., Tong, H., Bo, R., & Ni, M. (2014). Impact of communication failures on power system security and stability defense system. In *IEEE PES general meeting conference & exposition*, (pp. 1–5).
23. Unified Real Time Dynamic State Measurement, Power Grid Corp. (2012). Gurgaon: India Limited.
24. Appasani, B., & Mohanta, D. K. (2018). Co-optimal placement of PMUs and their communication infrastructure for minimization of propagation delay in the WAMS. *IEEE Transactions on Industrial Informatics*, *14*(5), 2120–2132.
25. Appasani, B., & Mohanta, D. K. (2017). Optimal placement of synchrophasor sensors for risk hedging in a smart grid. *IEEE Sensors Journal*, *17*(23), 7857–7865.
26. Simon, D. (2008). Biogeography-based optimization. *IEEE Transactions on Evolutionary Computation*, *12*(6), 702–713.
27. Freeman, R. L. (1997). *Radio system design for telecommunication*. Hoboken: Wiley.
28. Ghosh, D., Ghose, T., & Mohanta, D. K. (2013). Communication feasibility analysis for smart grid with phasor measurement units. *IEEE Transactions on Industrial Informatics*, *9*(3), 1486–1496.
29. Fcc.gov, '47CFR', 2016. Available: https://www.fcc.gov/general/rules-regulations-title-47. Accessed 22 Nov 2016.
30. Lehpamer, H. (2004). *Microwave transmission networks: Planning, design and deployment*. New York: Mc-Graw Hill.

31. Ebeling, C. E. (2004). *An introduction to reliability and maintainability engineering*. New York: Mc-Graw Hill.
32. Nadhvathuparambil, B., Valenti, M. C., & Feliachi, A. (2002). Communication delays in wide area measurement systems. In *Proc. Syst. Theory*, (pp. 118–122).
33. Khan, R. H., & Khan, J. Y. (2013). A comprehensive review of the application characteristics and traffic requirements of a smart grid communications network. *Computer Networks*, *57*(3), 825–845.
34. Baldwin, T. L., et al. (1993). Power system observability with minimal phasor measurement placement. *IEEE Transactions on Power Systems*, *8*(2), 707–715.
35. More, K. K., & Jadhav, H. T. (2013). *A literature review on optimal placement of phasor measurement units*, International Conference on Power, Energy and Control (ICPEC). (pp. 220–224). Dindigul, https://doi.org/10.1109/ICPEC.2013.6527654.
36. Gou, B. (2008). Optimal placement of PMUs by integer linear programming. *IEEE Transactions on Power Systems*, *283*(3), 1525–1526.
37. Gou, B. (2008). Generalized integer linear programming formulation for optimal PMU placement. *IEEE Transactions on Power Systems*, *23*(3), 1099–1104.
38. Deb, K. (2001). *Multi-objective optimization using evolutionary algorithms*. New York, Wiley.

Submit your manuscript to a SpringerOpen journal and benefit from:

► Convenient online submission
► Rigorous peer review
► Open access: articles freely available online
► High visibility within the field
► Retaining the copyright to your article

Submit your next manuscript at ► springeropen.com